AN ITERATIVE APPROACH FOR ESTIMATION OF THE DOPPLER CENTROID FREQUENCY FOR SAR DATA PROCESSING

Tomonori Kunito[1] and Yosuke Ito*[2]
[1]Postgraduate Student, Naruto University of Education
748 Takashima, Naruto-city, Tokushima Pref. 772-8502, Japan
E-mail: 10827031@naruto-u.ac.jp

[2]Professor, Naruto University of Education
748 Takashima, Naruto-city, Tokushima Pref. 772-8502, Japan
E-mail: ito@naruto-u.ac.jp

KEY WORDS: Iterative approach, SAR, Doppler centroid frequency, DELTA E method.

ABSTRACT: Precise processing parameters are necessary in order to produce high quality SAR images. The Doppler frequency at the time that the center of the SAR beam crosses the ground target is one of the most important parameters and is referred to as the Doppler centroid frequency (DCF). However, using a conventional method, it is difficult to accurately estimate the DCF using high-contrast SAR image data. The purpose of the present study is to develop an iterative approach by which to robustly estimate the DCF. Here, the Doppler ambiguity, which is referred to as an integer multiple of the PRF, is not considered because the SAR data is processed using only the yaw steering mode. The DELTA E method proposed by Madsen estimates the DCF based on an azimuth antenna pattern. This method is improved such that abnormal estimates are not obtained by introducing additional conditions that can detect improperly shaped power spectra in the azimuth direction. Few estimation results have been reported for high-contrast areas, in which the backscatter changes remarkably along the azimuth direction. In the proposed iterative approach, azimuth compression is carried out using an initial DCF. Since the mixed signal data within a synthetic aperture time are distinguished by azimuth compression, the DCF estimated from the azimuth-compressed image is close to the true value. The azimuth compression with the estimated DCF is repeatedly applied to the range-compressed SAR data, and the DCF is updated again. The iterative approach evaluates the convergence using a pair of DCFs estimated from the consecutive SAR images in order to decide the termination. The results of experiments using the raw data set of ALOS PALSAR for the Amazon rain forest, seacoast, and islands reveal that the proposed approach can be used to accurately and stably estimate the DCF.

1. INTRODUCTION

Precise processing parameters are necessary in order to produce high-quality SAR images for advanced detection methods such as radar interferometry. In particular, the Doppler frequency at the time that the SAR beam center crosses the ground target is one of the most important parameters and is referred to as the Doppler centroid frequency (DCF) (Cumming, 2005). However, using a conventional method, it is difficult to accurately estimate the DCF from high-contrast SAR image data. The purpose of the present study is to develop an iterative approach by which to robustly estimate the DCF. Here, the Doppler ambiguity, which is referred to as an integer multiple of the pulse repetition frequency (PRF), is not considered because the SAR data is processed using only the yaw steering mode. The DELTA E method proposed by Madsen estimates the DCF based on an azimuth antenna pattern (Madsen, 1989). The proposed method is applied to raw SAR data obtained by ALOS PALSAR. The convergence of the estimated DCFs is clarified experimentally.

2. IMPROVEMENT OF THE DELTA E METHOD

2.1 DCF Estimation Using the Energy Ratio

The Doppler magnitude spectrum is obtained by applying the Fourier transform to SAR data in the azimuth direction. The frequency of the peak gives an estimate of the DCF, assuming that the expected power spectrum is symmetric around the peak, the raw SAR data in the azimuth direction are digital signals sampled in the PRF. In general, the single-line spectrum is very noisy. The peak of a power spectrum with heavy noise is difficult to find. Therefore, the power spectrum is averaged over a number of range lines. The DCF estimation process uses the smoothed spectrum that clearly shows the peak. The DELTA E method can efficiently determine the peak and estimate the DCF. As shown in Figure 1, fs is a center frequency used to compute ΔE. Two sections with bandwidths Δf are defined at the high and low sides of fs. The energy E_1 in the high side and the energy E_2 in the low side are computed as integrations of the power spectrum in the corresponding section.

$$E_1 = \int_{f_s}^{f_s+\Delta f} p(f)df \qquad (1)$$

$$E_2 = \int_{f_s-\Delta f}^{f_s} p(f)df \qquad (2)$$

Next, the energy ratio is obtained by

$$\Delta E = \frac{E_1 - E_2}{E_1 + E_2} \qquad (3)$$

ΔE is a function of fs, which varies from $-PRF/2$ to $PRF/2$, and ΔE is computed at each fs. If $p(f)$ is symmetric in the neighborhood of the peak, then ΔE in its section becomes approximately linear, and the frequency fs_0 is such that $\Delta E = 0$. Consequently, fs_0 is the estimated DCF, $\hat{f}_{DC}$.

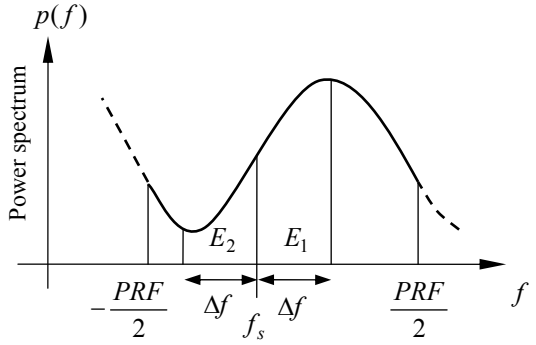

Figure 1. Integration sections in the DELTA E method.

2.2 Removal of the Estimated DCF Based on Nonlinear Degree

In general, the power spectrum in an area with homogeneous backscatter has a single peak. The DCFs in these areas can be estimated by applying the method described in Section 2.1. However, when an area with weak backscatter includes an area of strong backscatter, the power spectrum of this area may exhibit a distorted shape without a single peak. The DELTA E method is improved so as not to obtain abnormal estimates by introducing additional conditions, which can detect improper shapes of power spectra in the azimuth direction. The DCFs estimated using the DELTA E method greatly depend on the backscattering conditions in the area. In this section, power spectra with problems are shown, and a condition for eliminating such power spectra is presented. This method is referred to as the improved DELTA E method and introduces a new algorithm that uses a feature of ΔE to detect the improper shape of the power spectrum. The relationship between fs and ΔE is modeled by linear regression when the power spectrum of fs is greater than the mean. The total residual error is calculated by summing the squared error between the linear regression and ΔE. If the shape of power spectrum looks like a single peak, then the total residual error becomes small. Otherwise, the total residual error increases. Therefore, if the total residual error is greater than the threshold, then the DCF is not estimated. The threshold does not depend on the contrast in the area and is determined in preliminary experiments.

This section shows actual examples of power spectra in the SAR image shown in Figure 2(a). Since the power spectra in Figures 2(b) and 2(d) exhibit the single peaks, the DCFs can be estimated by the DELTA E method. The power spectrum in Figure 2(f) has two peaks and has an improper shape. The DCF cannot be accurately estimated by applying the DELTA E method to this type of power spectrum. The horizontal and vertical axes in Figure 3 denote the frequency fs and ΔE, respectively. The solid line in each graph indicates ΔE, and the dotted line shows the linear regression of ΔE. Figure 3(a) shows the ΔE curve computed from the power spectrum with the single peak in Figure 2(b) and its linear regression. The residual error becomes very small as both lines almost overlap. Figure 3(b) shows the ΔE curve computed from the power spectrum with an improper shape shown in Figure 2(f) and its linear regression. The residual error is clearly large in comparison with that shown in Figure 3(a). Therefore, the improved DELTA E method can remove the estimated DCF in this area.

3. ITERATIVE APPROACH TO THE ESTIMATION OF THE DCF

The DELTA E method provides almost no estimation results in the high-contrast area, in which the backscatter varies remarkably along the azimuth direction. In the present study, we propose a new iterative approach to estimate the DCF. Received signals that are spread along the azimuth direction are focused on a narrow area by the azimuth compression. For instance, the power spectra have a single peak caused by the azimuth compression, as shown in Figures 2(c), 2(e), and 2(g) which correspond to Figures 2(b), 2(d), and 2(f), respectively. Note that the power spectrum in Figure 2(g) has a single peak even if there are two peaks in Figure 2(f). Figure 3(c) shows the ΔE curve computed from the power spectrum in Figure 2(g) and its linear regression. This residual error becomes small because the power spectrum has a single peak. The DCF is estimated by applying the improved DELTA E method for the power spectrum in the range- and azimuth-compressed image. The estimated result is denoted by $\hat{f}_{DC}$, which is made to approach the true DCF by repeatedly applying the range-compressed image to the azimuth compression with $\hat{f}_{DC}$. The standard deviation of $\hat{f}_{DC}$ in the entire area becomes small as the iteration progresses. Figure 4 illustrates a flowchart of the proposed approach. First, the azimuth compression is performed using an initial DCF, such as 0 [Hz].

Next, the consecutive azimuth compression with the estimated DCF (f'_{DC}) is applied to the range-compressed SAR data. The DCF is estimated from the range- and azimuth-compressed image. The proposed method repeatedly performs estimation of the DCF and azimuth compression until the absolute difference between $\hat{f}_{DC}$ and f'_{DC} is less than the tolerance value, ε . Since $\hat{f}_{DC}$ is close to the true DCF, the iterative approach can provide a highly accurate DCF.

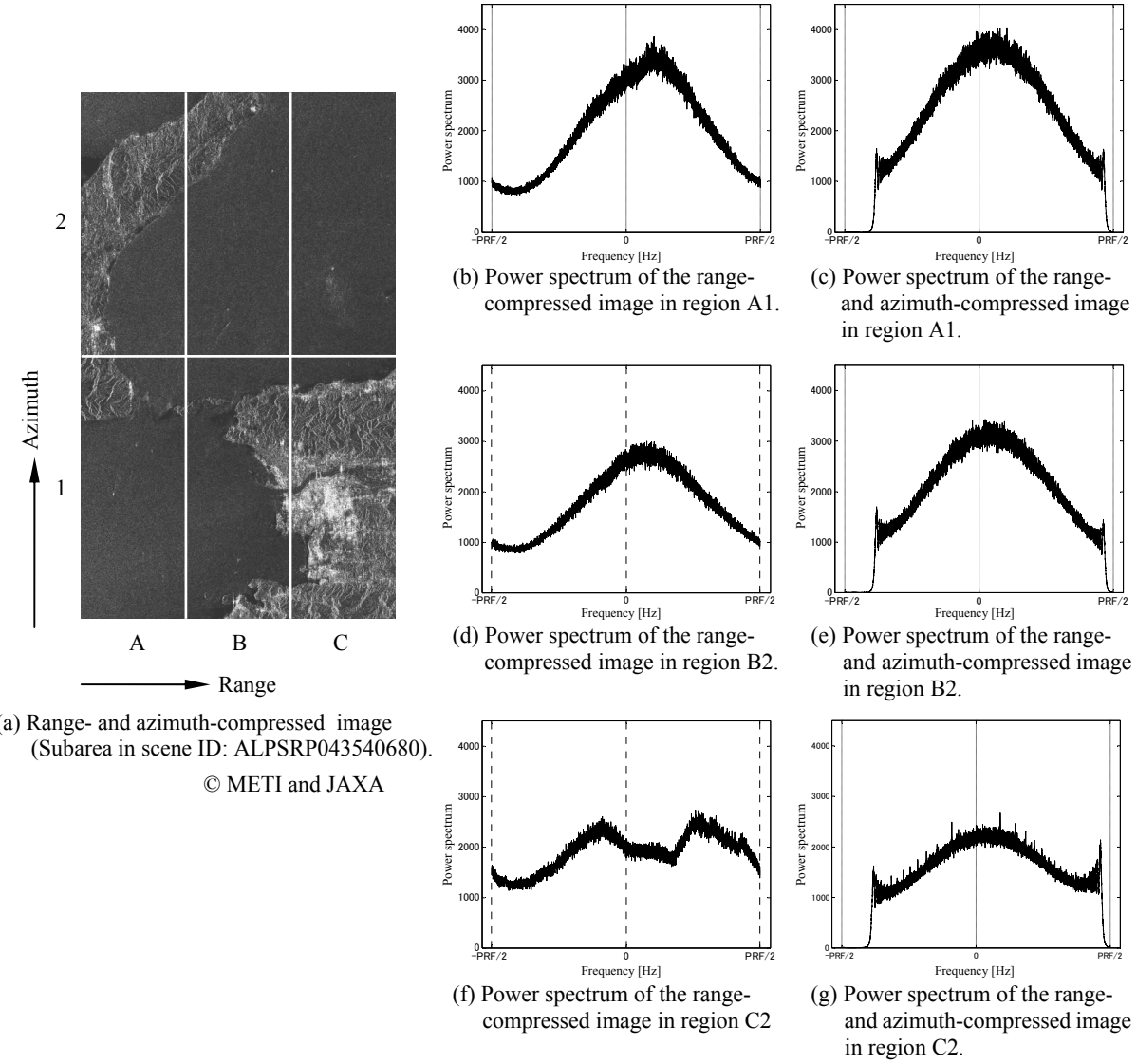

(a) Range- and azimuth-compressed image (Subarea in scene ID: ALPSRP043540680).

(b) Power spectrum of the range-compressed image in region A1.

(c) Power spectrum of the range- and azimuth-compressed image in region A1.

(d) Power spectrum of the range-compressed image in region B2.

(e) Power spectrum of the range- and azimuth-compressed image in region B2.

(f) Power spectrum of the range-compressed image in region C2

(g) Power spectrum of the range- and azimuth-compressed image in region C2.

Figure 2. Examples of power spectra in the azimuth direction obtained using ALOS PALSAR data.

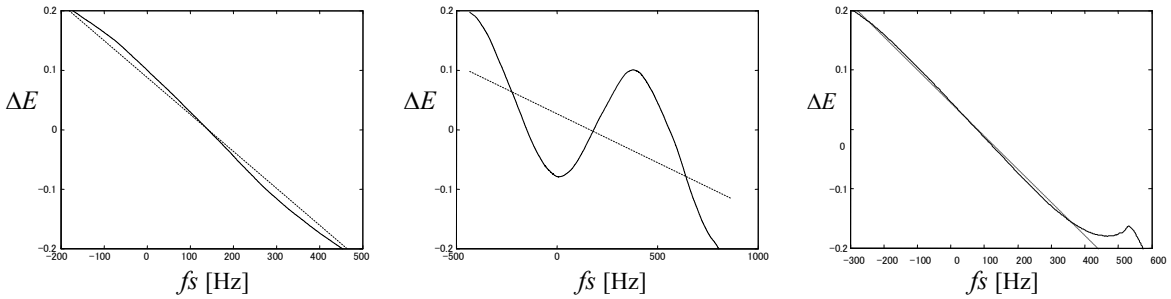

(a) ΔE obtained from the range-compressed image in region A1.

(b) ΔE obtained from the range-compressed image in region C2.

(c) ΔE obtained from the range- and azimuth-compressed image in region C2.

Figure 3. Residual error between ΔE and linear regression.

4. EXPERIMENTAL RESULTS

This section describes the experimental results of estimating the DCF. The block size for the improved DELTA E method is 1,024 pixels in the range direction and 8,192 lines in the azimuth direction. The intervals of the blocks are 100 pixels in the range direction and 1,000 lines in the azimuth direction. In the present study, the raw SAR data obtained by ALOS PALSAR are used in the experiments to estimate the DCFs by the proposed algorithm. Figure 5(a) shows the range-compressed image that convolves the raw SAR data with the range reference function. Figure 5(b) shows the focused SAR image that convolves the range-compressed image (Figure 5(a)) with the range cell migration correction and the azimuth reference function (Sandwell, 2008).

Scatter diagrams are depicted in order to analyze the change of the estimated DCF in the range direction, as shown in Figure 6. The horizontal and vertical axes in Figure 6 denote the range pixel number and the estimated DCF, respectively. The expression in each diagram is the linear regression computed from the estimated results. The white and black dots denote the estimated DCFs for the SAR images in Figure 5. The black dot in each diagram denotes rejection due to exceeding the tolerance of the total residual error defined in Section 2.2. Figure 6(a) indicates the distribution of the DCFs estimated from the range-compressed image. Since the dispersion of the estimated DCFs is wide, the standard deviation of the dispersion becomes large and the number of rejected points increases. Consequently, the estimated DCFs are considered to be unreliable. Figure 6(b) shows the distribution of the DCFs estimated from the first azimuth-compressed image with $f'_{DC} = 0$ [Hz]. The standard deviation is smaller than that of Figure 6(a), and the number of rejected points decreases as well. However, f'_{DC} is assumed to be 0 [Hz] in the first azimuth compression. It is necessary to apply the azimuth compression with the estimated DCF to the range-compressed image again. Figure 6(c) indicates the distribution of the DCFs estimated from the second azimuth-compressed image with f'_{DC} based on the regression line, as shown in Figure 6(b). As the count of the azimuth compression increases, the coefficients in the linear regression for the adopted DCFs become stable.

Finally, convergence of the estimated DCF is clarified by applying the iterative approach to three scenes obtained by ALOS PALSAR. The locations of ALPSRP043540680, ALPSRP037120700, and ALPSRP023057030 are Awaji island in Japan, as shown in Figure 5, Mt. Fuji and Suruga Bay in Japan, and an area of the Amazon rainforest, respectively. Figure 7 shows the estimated DCFs at range No. 3500 for the azimuth compression count where the zero count indicates the range compression only. The trends of the estimated DCF for the azimuth count in three scenes are similar. The absolute DCF estimated from the range-compressed image is slightly larger than the converged value. The estimated result is the value between the true DCF and zero because f'_{DC} is assumed to be 0 [Hz] in the first azimuth compression. As the count of azimuth compression increases, the estimation values become stable in three scenes. Figure 8 shows the standard deviations of the estimated DCFs in each azimuth compression step. The image of the Amazon (ALPSRP023057030) has low contrast. The standard deviations derived from the image are unchangeable regardless of the azimuth compression count. However, accurate estimation results cannot be obtained because the standard deviations of the DCFs estimated from only a high-contrast range-compressed image, such as ALPSRP043540680, or ALPSRP037120700. On the other hand, the standard deviation of the DCFs estimated from the azimuth-compressed image

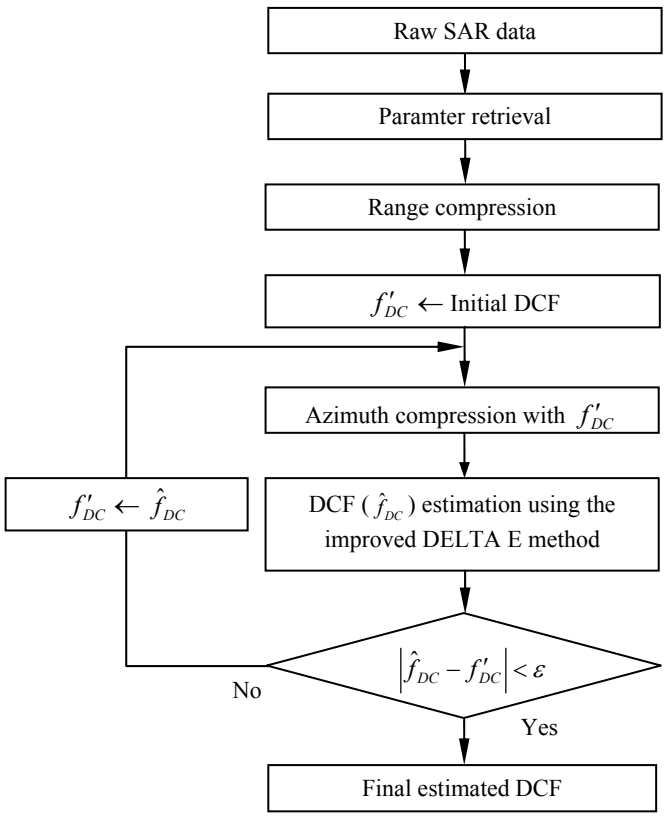

Figure 4. Flowchart of the iterative approach.

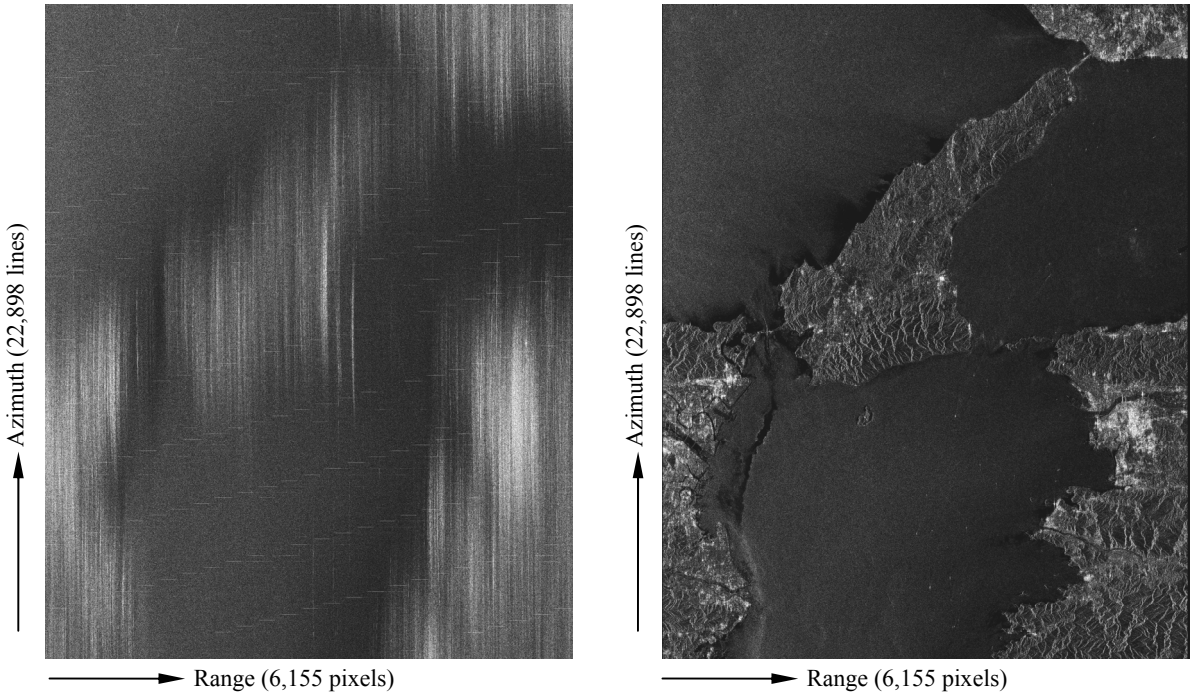

(a) Range-compressed image. (b) Range- and azimuth-compressed image.

Figure 5. SAR images of PALSAR (Scene ID: ALPSRP043540680, Mode: FBS-HH, Ascending orbit, Off-nadir: 21.5°, Date: 18 Nov. 2006, Center location: 34° 19' 32" N, 134° 55' 30", Awaji island, Japan).

obviously decreases. Consequently, high-precision DCFs can be experimentally obtained by iteratively applying azimuth compression with the estimated DCF.

5. CONCLUSIONS

In the present study, a method was proposed that robustly estimates the DCF based on the shape of the power spectrum in the azimuth direction and its usefulness was proven experimentally. The improved DELTA E method was capable of eliminating abnormal estimates by introducing an additional procedure to detect improper shapes in the power spectrum. Furthermore, the iterative approach was used to evaluate the estimated DCF. As a result of experiments using the raw data set of ALOS PALSAR, the estimated value was found to approximately converge by adopting the proposed approach. In order to support the SAR, which does not have the yaw steering mode, it is necessary to develop a method by which to obtain the ambiguity for the PRF of the DCF.

ACKNOWLEDGMENTS

The SAR data were provided under the second ALOS research announcement of the Japan Aerospace Exploration Agency.

REFERENCES

Cumming, I. G. and Wong, F. H., 2005. Digital Processing of Synthetic Aperture Radar Data, Artech House, Norwood, MA, pp.483–565.

Madsen, S. N., 1989. Estimating the Doppler centroid of SAR data, IEEE Transactions on Aerospace and Electronic Systems, Vol.25, No.2, pp.134–140.

Sandwell, D., 2008. SAR image formation: ERS SAR processor coded in MATLAB, http://topex.ucsd.edu/insar_notes/04_SAR_image_formation.pdf (accessed 5 August 2011)

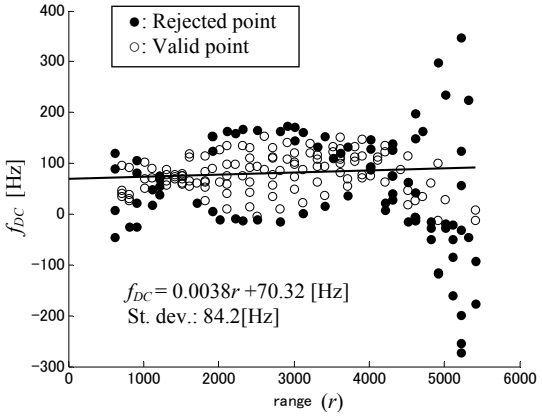

(a) DCFs estimated from the range-compressed image.

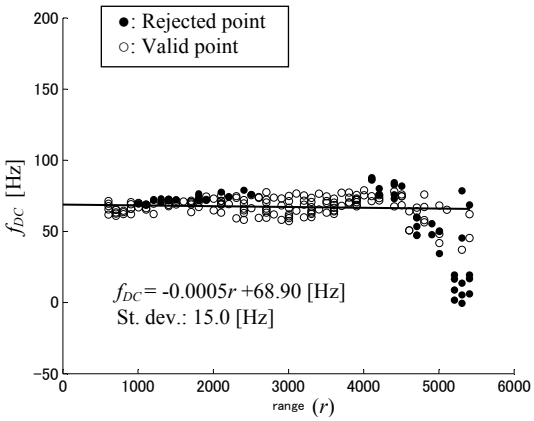

(b) DCFs estimated from the first azimuth-compressed image with $f'_{DC} = 0$ [Hz].

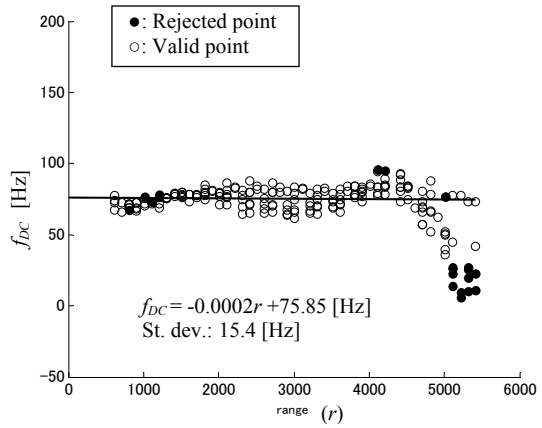

(c) DCFs estimated from the second azimuth-compressed image with the first estimated f'_{DC}.

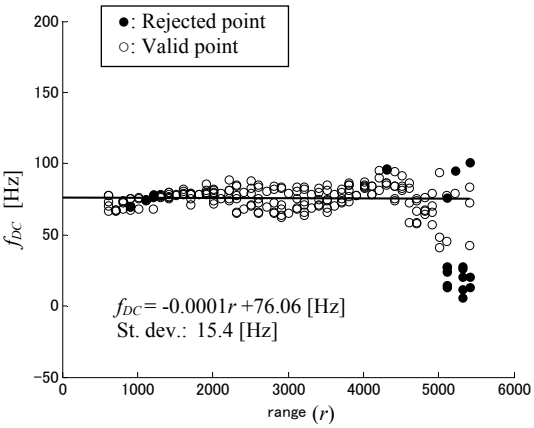

(d) DCFs estimated from the third azimuth-compressed image with the second estimated f'_{DC}.

Figure 6. Distribution of estimated DCFs.

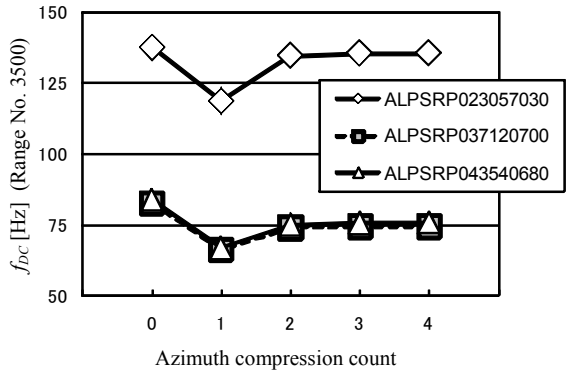

Figure 7. Results for estimated DCFs using ALOS PALSAR data.

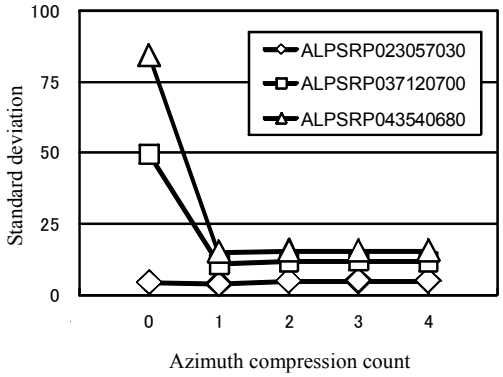

Figure 8. Standard deviations of estimated DCFs using ALOS PALSAR data.